Available online at www.eccomasproceedia.org
Eccomas Proceedia COMPDYN (2021) 5318-5330

ECCOMAS
Proceedia

COMPDYN 2021
8th ECCOMAS Thematic Conference on
Computational Methods in Structural Dynamics and Earthquake Engineering
M. Papadrakakis, M. Fragiadakis (eds.)
Streamed from Athens, Greece, 28 - 30 June 2021

POWDER SNOW IMPACT OF TALL VIBRATING STRUCTURES

Andrin Caviezel[1], Stefan Margreth[2], Kseniya Ivanova[1], Betty Sovilla[2] and Perry Bartelt[1]

[1]WSL Institute for Climate, Extremes and Alpine Natural Hazards CERC
Davos Dorf, Switzerland
e-mail: {caviezel,ivanova,bartelt}@slf.ch

[2] WSL Institute for Snow and Avalanche Research SLF
Davos Dorf, Switzerland
e-mail: {margreth,sovilla}@slf.ch

Abstract. *Tall structures play an important role in the economic well-being of mountainous regions. They serve to distribute hydroelectric energy (power line transmission towers), generate tourist income (cableway pylons) and protect important infrastructure from natural hazards (trees). It is not uncommon for these structures to be destroyed by the air-blast of a powder avalanche. In this paper we investigate the shock response spectra of an asymmetric steel structure subjected to powder avalanche impact. We perform a spectral analysis of measured accelerations in the in-plane (avalanche flow) and cross-plane (normal to avalanche flow) directions. The structural eigenfrequencies in each direction are likewise calculated using a simple finite element model consisting of three-dimensional beam elements. Mode superposition is then used to reconstruct the measured accelerations, velocities and displacements in order to identify the magnitude and duration of the powder avalanche loading. From the analysis we find that the powder avalanche must contain high-frequency, short-duration blasts ($f > 2$ Hz) of moderate magnitude ($p \approx$ 1-10 kPa). High frequency blasts are also present in the cross-plane, transverse flow direction. This result, however, does not exclude the existence of longer duration blasts, which, because of the frequency mismatch, cannot excite the measurement pylon. It appears the high-frequency content of the cloud attenuates to endanger low-frequency structures ($f \approx$ 1 Hz) such as trees at the lateral edges of the flow, or hanging cables located well above the core. The shock response of a specific structure therefore depends on its location relative to the avalanche core, depending on how the blast-structures dissipate in time and space. Because the powder cloud contains a wide range of blast frequencies, tall structures are vulnerable to the action of the powder cloud, even if they are located well outside the avalanche core.*

Keywords: Powder Snow Avalanche, Impact, Dynamic Magnification, Power Transmision Towers, Pylons, RAMMS

ISSN:2623-3347 © 2021 The Authors. Published by Eccomas Proceedia.
Peer-review under responsibility of the organizing committee of COMPDYN 2021.
doi: 10.7712/120121.8868.19112

1 INTRODUCTION

A longstanding problem in natural hazards engineering has been to predict the action of snow avalanches on power transmission towers and pylons. These are thin, tall structures, that are exposed to both the impact of the dense avalanche core and powder cloud (Figs. 1 and 2). The avalanche core is composed of clumps and clods of compacted snow with bulk densities reaching 500 kg/m^3 or even higher (Fig. 3). The avalanche core is primarily a surface flow governed strongly by terrain and slope properties (steepness, roughness, vegetation, gullies, channels, etc) [1]. Although engineers can often position transmission towers and pylons outside the reach of the flow core, exploiting natural terrain features such as elevated ridges and knolls, they are nonetheless subjected to the wind blast of the airborne powder cloud.

Figure 1: Left: The front of a powder snow avalanche. Photograph taken at the Swiss experimental avalanche dynamics site in 2003. The avalanche is moving at a speed between 40-50 m/s. Note the turbulent billow and cleft structures an indication of velocity fluctuations. Right: A powder avalanche overturned this power transmission mast in January 2018. The mast is located in the runout zone of the Val Barcli avalanche track, Zernez, Switzerland. The conductors are still attached to the mast which appears to be severely damaged near the foundation. Note the mangled and twisted truss elements near the foundation suggesting a multi-dimensional loading. The photograph appeared in the newspaper Engadiner Post, January 24th, 2018. The transmission line belongs to the Engadiner Kraftwerke AG (EKW).

The powder cloud consists of suspended ice-dust; it is created when both dense particles and ice-dust are ejected from the avalanche core into the surrounding air, often quickly and to great heights [1]. The suspended dust remains airborne while the larger particles eventually return back to the core. The difference in particle sizes thus leads to a natural separation between the core and cloud. The cloud is created from the core and during the formation phase is continually supplied with mass and momentum from the core. It can reach significant speeds. More importantly, once airborne the flow of suspended ice-dust is free from the terrain and will essentially travel in the initial direction defined by the core/cloud momentum exchange. Thus, while the core is a surface flow, the cloud is an inertial, airborne flow. At formation the flows are combined, but the flows can separate, flow in different directions and velocities and therefore can inundate larger areas.

Figure 2: An avalanche displaced and tilted this cableway mast in East Tirol, Kals, Austria. The mast itself was not damaged and could be brought back into an upright position. The picture appeared in the Dolomitenstadt.at online magazine on November 21, 2019.

Transmission towers and pylons are vulnerable to the action of the powder cloud. For one, because the powder cloud applies wind loadings at significant heights above the ground. The primary purpose of these structures is to carry cables above ground. They are designed for vertical loads and horizontal wind loads. As such, heavy, cable supporting sub-structures are often located well above the ground, Fig. 2. Mass is therefore not equally distributed over the height, but often concentrated near the top of the structure. This makes masts and pylons particularly vulnerable to dynamic loads. If this mass is excited by the avalanche impact, large internal stresses can be generated by the external loading. Another problem is that the cables between towers can also be impacted by the powder cloud. That is, the towers can escape the powder blast, but the cables are often subjected to pressures larger than the wind load. The impact of the cables creates internal stress/deformation waves that propagate back and forth between the towers, with a magnitude and frequency dependent on the elasticity and cross-sectional mass of the cables [2]. This leads to concentrated, dynamic loads on the towers, again at some distance above the ground. Thus, powder avalanches can both directly and indirectly produce dynamic loads on tall tower-type structures (Fig. 4).

The purpose of this paper is the following. We first would like to identify the duration and magnitude of powder avalanche impact loadings on tall, thin structures. This information is the prerequisite for performing a dynamic structural engineering analysis for both man-made structures as well a natural structures such as trees [3]. We do this by back-calculating measured accelerations on a tall, asymmetric structure with known cross-section and material properties. For this purpose we develop a simple three-dimensional finite element beam model. Thus, we are able to approximate both longitudinal and transverse loadings arising from the powder cloud

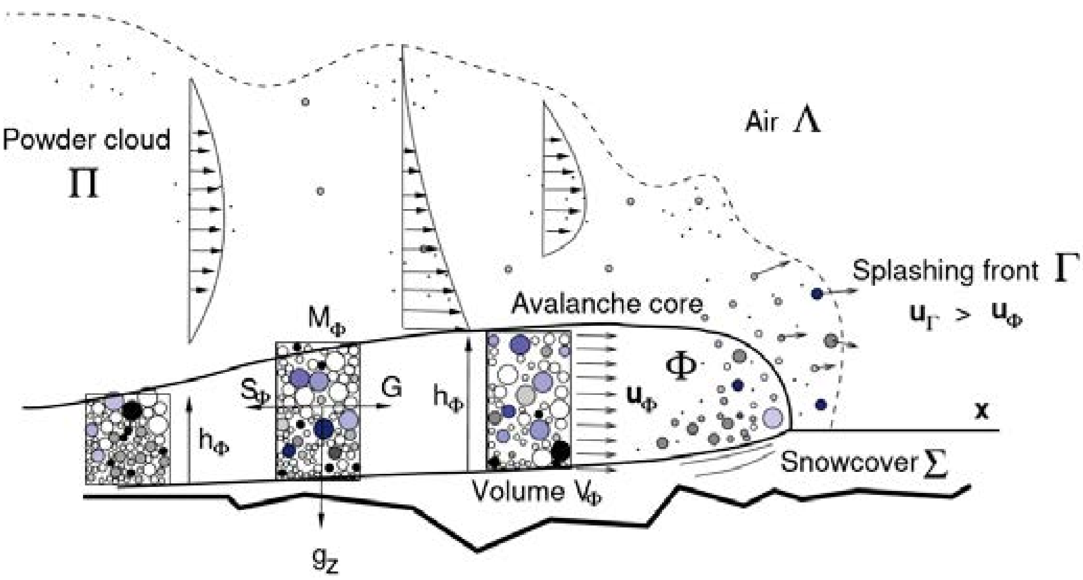

Figure 3: Flowing avalanche core Φ and powder cloud Π. Avalanche dynamics models predict the movement of the core and cloud in general terrain. The core contains granular mass in the form of clumps of snow. The cloud contains suspended ice-dust. The layers are not separate, but overlaid and mixed. The height of the core is defined by the location of the highest clump of snow; that is, it includes saltating particles at great heights in the powder cloud. A splashing front exists at the front of the avalanche.

impact. We perform a modal analysis to identify the duration, location and magnitude of the blast [4]. We then apply a mixed flowing/powder avalanche model to calculate the destruction of the mast to demonstrate the important contribution of the dynamic powder blast to overall avalanche loading. Clearly, the primary objective of this paper is to underscore the necessity of including both (internal) inertial forces and (external) impulsive forces when calculating the response of tall structures to powder avalanche impact.

2 ACCELERATION MEASUREMENTS and FE-MODAL ANALYSIS

Acceleration measurements on the 20 m high, tubular steel pylon at the Swiss Vallée de la Sionne test site are used to determine the duration and intensity of powder loadings [5, 6]. The width of the pylon is approximately w = 0.6m, with bevelled edges; in the direction of avalanche flow the pylon is 1.6 m long. Accelerometers are fixed on the pylon at four heights (3.8 m, 7.8 m, 12.3 m, 16.3 m) and measure accelerations in both the longitudinal (avalanche direction) and transverse (perpendicular to flow) directions. The pylon is fixed rigidly to the ground via a concrete sub-structure and can be considered a fixed-end cantilever. Because of internal stiffness elements and variable section thickness (1-3 cm), the moments of inertia can vary with height somewhat. Values at the midsection are stated here, I_Y = 0.0042 m^4 and I_Z = 0.0125 m^4. The flexural rigidity of the pylon is subsequently a factor 3 lower in the transverse direction. The modulus of elasticity and density for steel are applied in the analysis, E = 200 GPa and ρ = 8000 kg/m^3, respectively.

Measured accelerations in the transverse and longitudinal directions are depicted in Fig. 5. The measurements reveal (1) Within six seconds the pylon was struck by a series of short duration blasts lasting less than a fraction of a second, between 0.25 s and 0.50 s. (2) Higher accelerations are measured in the transverse (less stiff) direction, (3) the magnitude of the accelerations at the highest location (16.3 m) reach 10 g in the transverse direction and 4 g in the

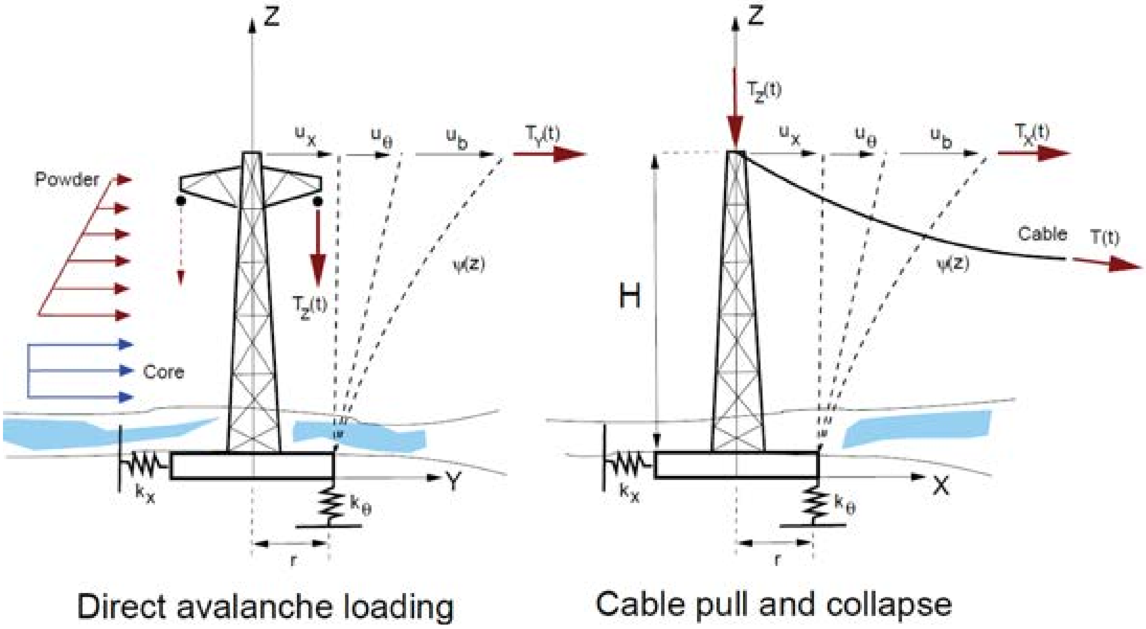

Figure 4: We consider two loading cases: 1) The avalanche core and cloud directly impacts the mast. 2) The mast is outside the reach of the core and cloud and the avalanche impacts only the cables, causing pull and collapse forces on the mast. The avalanche impacts the mast in transverse Y-direction producing bending moments around the X-axis. The X-direction runs parallel to the cable. Cable impact induces pulling forces $T_X(t)$ in the X-direction and collapse forces $T_Z(t)$ in the Z-direction. These induce bending moments around the Y-axis. A third loading case is when both the mast and cables are struck by the avalanche.

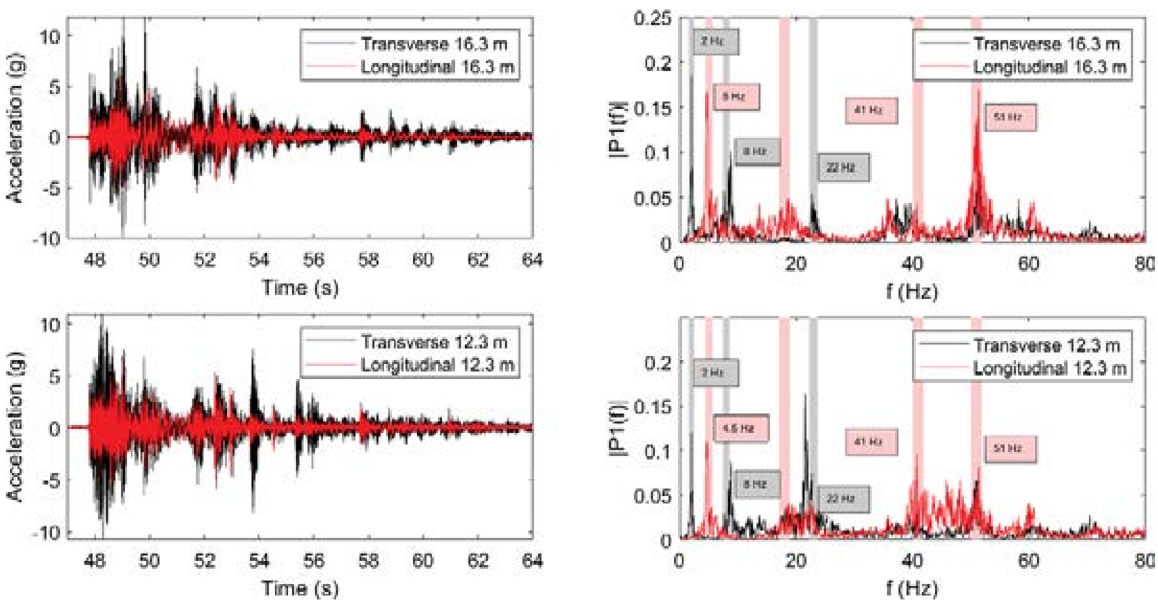

Figure 5: Left: Measured accelerations at heights 16.3 m and 12.3 m in the transverse (black) and longitudinal (red) directions. Right: Frequency analysis of the measured accelerations. The three lowest eigenfrequencies in longitudinal direction are 5 Hz, 18 Hz and around 40 Hz; in the transverse direction 2 Hz, 8 Hz and 18 Hz.

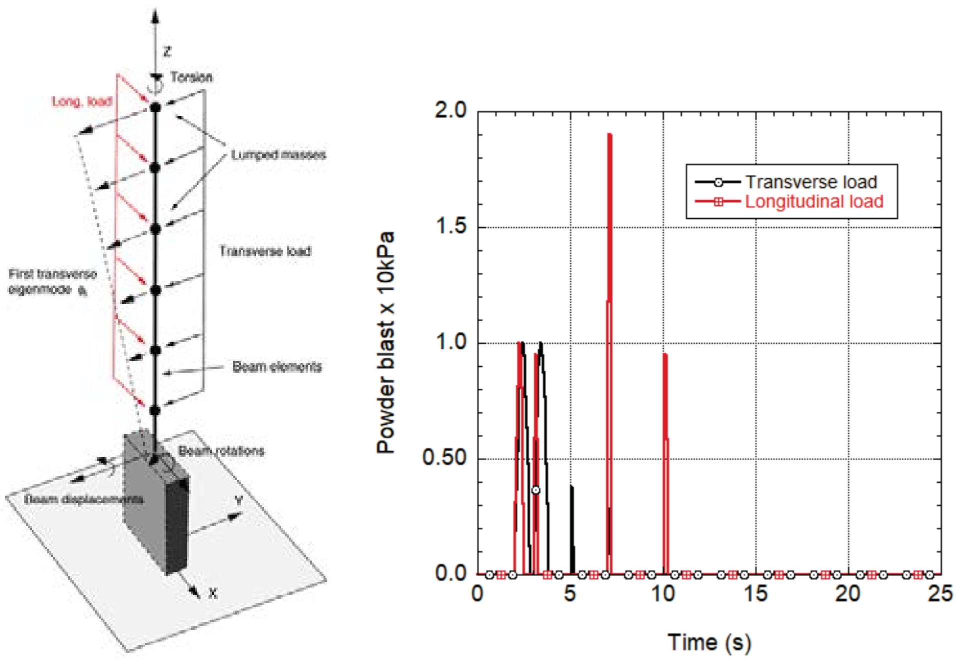

Figure 6: Left: Three-dimensional finite element beam model displaying the transverse and longitudinal directions. The finite element model is used to determine the eigenmodes of the structure. Right: A powder loading is applied to the structure as a series of random pulses.

longitudinal direction and finally (4) the intensity of the blast is clearly highest at or near the avalanche front.

We performed a discrete Fourier transform using the standard fast Fourier transform (FFT) algorithm [7] to identify the eigenfrequencies. Figure 5 shows raw data streams and its according FFTs without applying any data filtering. Likewise, we developed a simple finite element model consisting of three-dimensional beam elements to model the pylon structure (Fig. 6). The finite element model consisted of 7 elements, 8 nodes (48 DOFs). We calculated all n = 48 eigenvalues (ω_n) and eigenvectors (ϕ_n) using MAPLE [8]. Measured and calculated eigenfrequencies are presented in Table 1.

Mode no.	Longitudinal X-direction Eigenfrequency ϕ_z (Hz) Measured/FE	Transverse Y-direction Eigenfrequency ϕ_y (Hz) Measured/FE
1	5.0 / 5.1	2.0 / 1.9
2	18.0 / 18.5	8.0 / 8.8
3	41.0 / 41.5	18.0 / 21.3

Table 1: Longitudinal and transverse eigenfrequencies of the impact pylon.

The orthogonality properties of the eigenvectors can be used to uncouple the general equations of motion to arrive at a series of n=3 differential equations in the longitudinal and transverse directions [4],

$$M_n\ddot{Y}_n + C_n\dot{Y}_n + K_nY_n = P_n(t) \tag{1}$$

where

$$M_n \equiv \phi_n^T m\phi_n \qquad K_n \equiv \phi_n^T k\phi_n \qquad P_n \equiv \phi_n^T p(t) \tag{2}$$

are the generalized mass (FE mass matrix m), stiffness (FE stiffness matrix k) and load (FE load vector $p(t)$). The damping C_n is determined using the usual method of assigning a damping ratio for each mode n. For the mode-superposition method we took the three lowest eigenfrequencies in the longitudinal and transverse direction and therefore solved a system of six ordinary differential equations to find the dynamic response. Higher frequencies were not included in the analysis.

We matched the experimental results by selecting short duration blasts arranged randomly over the six second interaction time. The load $p(z, t)$ acted over the entire pylon height. The magnitude of the load did not change between the longitudinal and transverse directions p_0 = 5 kPa. The avalanche core was assumed to act only on the lower region of the pylon ($h < 5$ m). The measurements appear to be strongly damped and we selected an appropriate damping ratio for each mode.

In order to capture measurements it was necessary to apply several high-frequency blasts of duration 0.25 s $\leq \Delta t \leq$ 0.5 s (Fig. 6). We applied these loads homogeneously over the entire height. The blasts must be applied in both flow and cross-flow directions. The fact that the pylon structure is asymmetric, and therefore has two dissimilar first bending mode eigenfrequencies, is helpful to quantify the frequency content and blast magnitude in both directions. For the blast loading we found the frequency content and intensity to be similar (Fig. 7).

It would be entirely wrong to conclude the powder cloud contains *only* turbulent structures of duration 0.25s to 0.50s (2Hz - 4Hz). These pulses exist at the eigenfrequency of the pylon, and therefore the pylon reacts to them. Lower frequency (longer duration) pulses could exist in the cloud, but the pylon would not react to them. These pulses would therefore not be seen in the measurements.

Of considerable importance is the fact that we applied significant core loadings to the structure at the same time as the powder blast. The magnitude of the acceleration response, however, was not dominated by the magnitude of the long-duration core load (p = 60 kPa), rather by the short duration of the powder blast, especially in the transverse direction. Using the model it was possible to obtain similar accelerations in both the longitudinal and transverse directions, at different heights. Clearly, the comparison between the measurements and model results could be optimized to obtain the exact magnitude and load timing. We show that with a relatively simple load model a reasonable and good quantitative fit to the experiments can be achieved. Remarkable is the model prediction of the three lowest eigenfrequencies in each direction.

Finally, we note that we applied the powder blasts over the entire pylon. Only in this way could we match the measured accelerations. This result indicates that the pulses have considerable height (20m) in the Z-direction, larger than the pulse wavelength in the $X-$ and $Y-$ directions. Vorticity in the cloud must therefore not be distributed equally in all directions.

3 RAYLEIGH ANALYSIS with AVALANCHE DYNAMICS SIMULATIONS

To reinforce the idea that the duration and magnitude of the powder blast contributes a large part to the total structural load, we performed a simple Rayleigh analysis, using a method developed by Wolf [9]. In this section we investigate two of the largest snow avalanches ever recorded at the Swiss Vallée de la Sionne test site. These are the avalanches of the 10th of February and 25th February, 1999. Both avalanches are documented in the SLF internal report No. 732 entitled *Lawinendynamik-Versuchsgelände Vallée de la Sionne–Arbaz, Wallis. Schlussbericht Winter 1998/1999.* These avalanches clearly impacted the pylon structure with a significant core loading.

We construct an equivalent one-dimensional model of the mast (Rayleighs method) given by

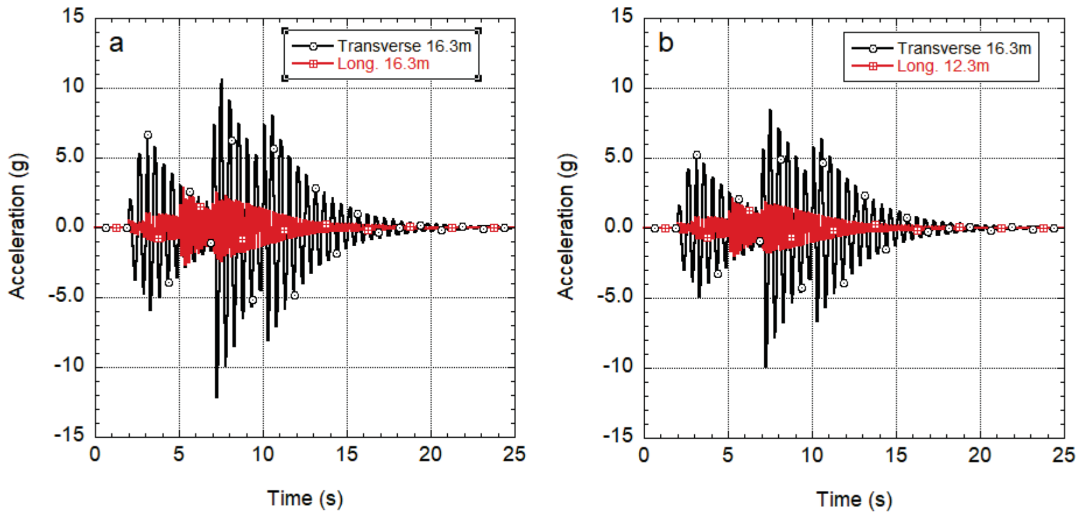

Figure 7: Results of the FE mode-superposition analysis. Transverse (black) and longitudinal (red) accelerations. a) z = 16.3 m. b) z = 12.3 m. The calculations are damped with first mode damping ratios of ξ_n = 0.02.

the dynamic equation

$$M\ddot{u}(t) + Ku(t) = P(t) \tag{3}$$

where M, K and P are the effective mass, stiffness and loading values. The deformation at the top of the structure $z = H$ is $u(t)$. For this simple analysis we neglect structural damping. We use the analytical function (see [4])

$$\psi(z) = 1 - \cos\frac{\pi z}{2H}. \tag{4}$$

to model the bending displacement. The effective mass and loading are then found,

$$M = \int_0^H m(z)\left(\psi(z)\right)^2 dz \qquad P(t) = \int_0^H p(z,t)\psi(z)dz. \tag{5}$$

The mass distribution of the steel structure is given $m(z)$; the external avalanche loading $p(z,t)$. The effective bending stiffness (flexural rigidity $EI(z)$) is given by

$$k_b = \int_0^H EI(z)\left(\frac{d^2\psi}{dz^2}\right) dz \tag{6}$$

which we modify to include foundation effects according to the procedure of Wolf [9],

$$K = \frac{k_b}{\left[1 + \frac{k_b}{k_x} + \frac{k_b H^2}{k_\theta r^2}\right]} \tag{7}$$

where the parameters k_x, k_b and r characterize the foundation stiffness. The dimensions of the pylon (width 0.6 m, length 1.6 m, avg. plate thickness 25 mm) were used to approximate the flexural rigidity of the tubular steel structure EI = 3.5 GNm^2. This also provided the approximate mass per running height of the pylon (m = 550 kg/m). We considered a soil strength of k_x = k_x = 75 MN/m. This produced a vibration frequency ω = 12.2 rad/s (f = 1.95 Hz), in good agreement with the finite element model and the acceleration measurements. The natural vibration frequency of the pylon on an absolutely rigid foundation is ω = 25.0 rad/s (f = 4 Hz).

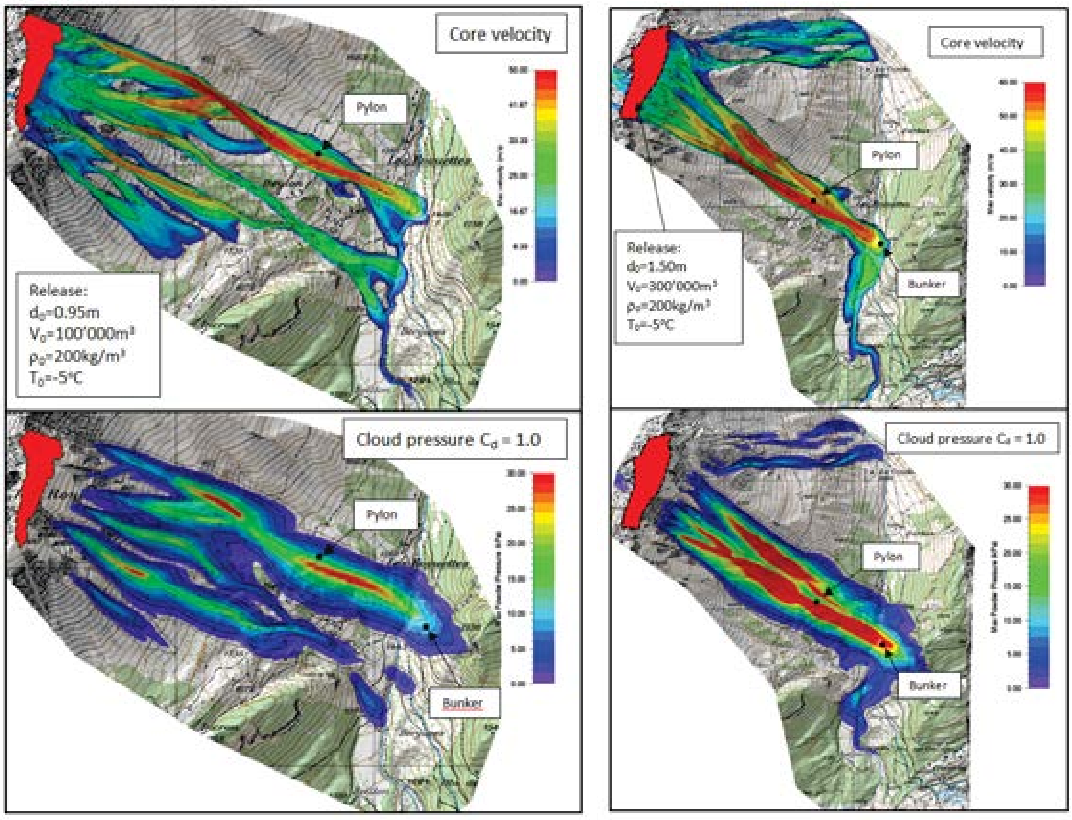

Figure 8: Vallee de la Sionne, 1999. Calculated core velocities and powder cloud impact pressures (**RAMMS**) for two large powder avalanches that occurred on 10.2.1999 and 25.2.1999. The calculated pressures are around 35 kPa (C_d = 1).

We first simulated the avalanche events with the **RAMMS** software [10] to determine the core and powder cloud loadings (Fig. 8). An overview of the simulation results is contained in Table 2. Pre- and post event photogrammetric measurements were used to derive the mass balance of both avalanches. The location and extent of the release zones are also defined according to the photogrammetric measurements. The fracture depths d_0 and release volumes V_0 likewise correspond to the experimental observations.

The calculated avalanches reach peak leading-edge velocities of 60 m/s (10.2.1999) and 80 m/s (25.2.1999), close to the observed values (see report). The calculated runout distances correspond to the observations. The avalanche of 25.2.1999 inundated the forested area behind the bunker with pressures large enough to knock down trees (observed and calculated). The powder pressure of the 25.2.1999 avalanche is considerably higher than the avalanche of 10.2.1999. This is in large part due to the fact that the core of 25.2.1999 avalanche impacted the mast directly, whereas the core of the 10.2.1999 avalanche flowed past the pylon on the orographic right side, reducing the magnitude of the calculated powder pressures. This fact suggest large transverse loadings on the structure for the second avalanche. The calculation results where used to construct core and cloud loading that are shown in Fig. 9. Note that the core of the 25.2.1999 avalanche struck the mast at a higher level as it flowed on the deposits of the 10.2.1999 avalanche.

The first surprising result of the Rayleigh analysis is that the powder avalanche load contributes significantly to the effective avalanche loading in both the longitudinal and transverse directions (Fig. 10). The effective loading of the 25.2.1999 avalanche is a factor 5 times larger

Vallée de la Sionne February 1999	10.2.1999	25.2.1999
Release height d_0 (m)	0.98/0.95	1.50/1.50
Measured release volume V_0 (m^3)	104'000/105'650	316'000/315'125
Release temperature T_0 (^{o}C)	-5	-5
Release density ρ_0 (kg/m^3)	200	200
Snowcover gradient Δh_Σ (cm/100m)	5	5
Temperature gradient ΔT_Σ (^{o}C/100m)	0.5	0.5
Calculated erosion volume (m^3)	607'300	1'265'000
Calculated core mass to cloud (t)	33'110	75'100
Cloud deposition volume (m^3)	74'000	167'000
Measured deposition volume (m^3)	760'000	1'710'000
Calculated deposition volume (m^3)	786'950	1'747'125

Table 2: Mass balance of Vallée de la Sionne avalanches February 1999. The size and location of the release zone are taken directly from the experimental report. The total measured deposition volume is compared to the calculated deposition volume which is the sum of the simulated release, erosion and powder cloud deposition volumes.

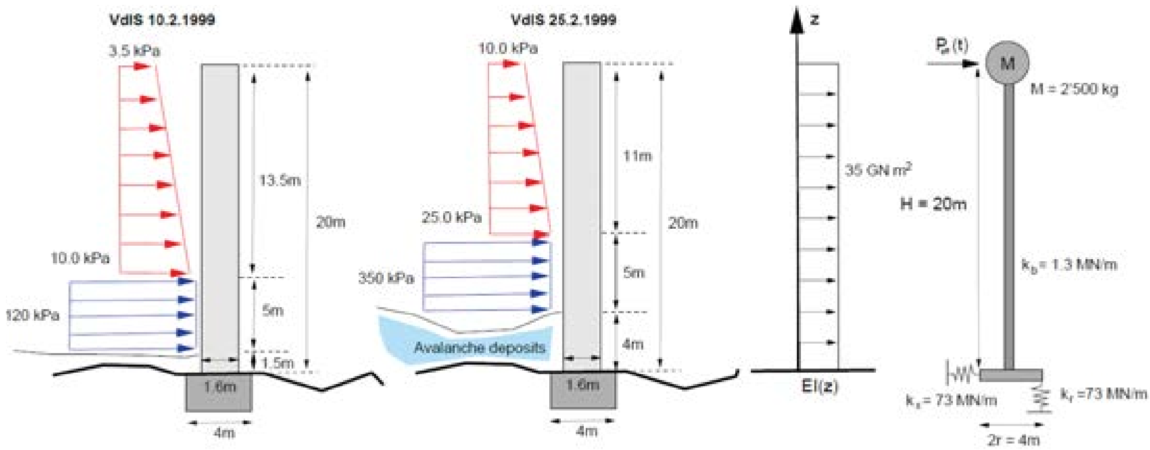

Figure 9: Calculation model of the VDLS pylon for two avalanches (10.2.1999 and 25.2.1999) in 1999. The second avalanche destroyed the pylon. The two loadings produce two different effective loadings $P_{\text{eff}}(t)$.

than the avalanche of 10.2.1999 – although the pressure loading from the core and cloud vary only by a factor two. This is due in part to the stronger powder cloud pressure of 25.2.1999, but also due to the fact that the core load is elevated 4 m from the base of the pylon. For the avalanche of 25.2.1999 the effective loading increases from $P_{\max}$ = 150 kN to peak impact pressures of $P_{\max}$ = 300 kN; that is, the effective loading essentially doubles. Note that the duration of the core and powder loadings differ - the core loading is of longer duration (15s) than the powder loading (<1 s). The Rayleigh analysis effectively quantifies the effect of the loading elevation.

Another interesting result of the Rayleigh analysis is that the elastic limit (2000 $\mu\epsilon$) is reached because of the transverse impact. Strains from the transverse loading are approximately 4 times higher than from longitudinal loading (500 $\mu\epsilon$), see Fig. 10c. The calculated accelerations in the transverse direction have a higher order of magnitude that the experimental measurements (15 $g > 5$ g), but are also longer lasting, suggesting a more intense impact.

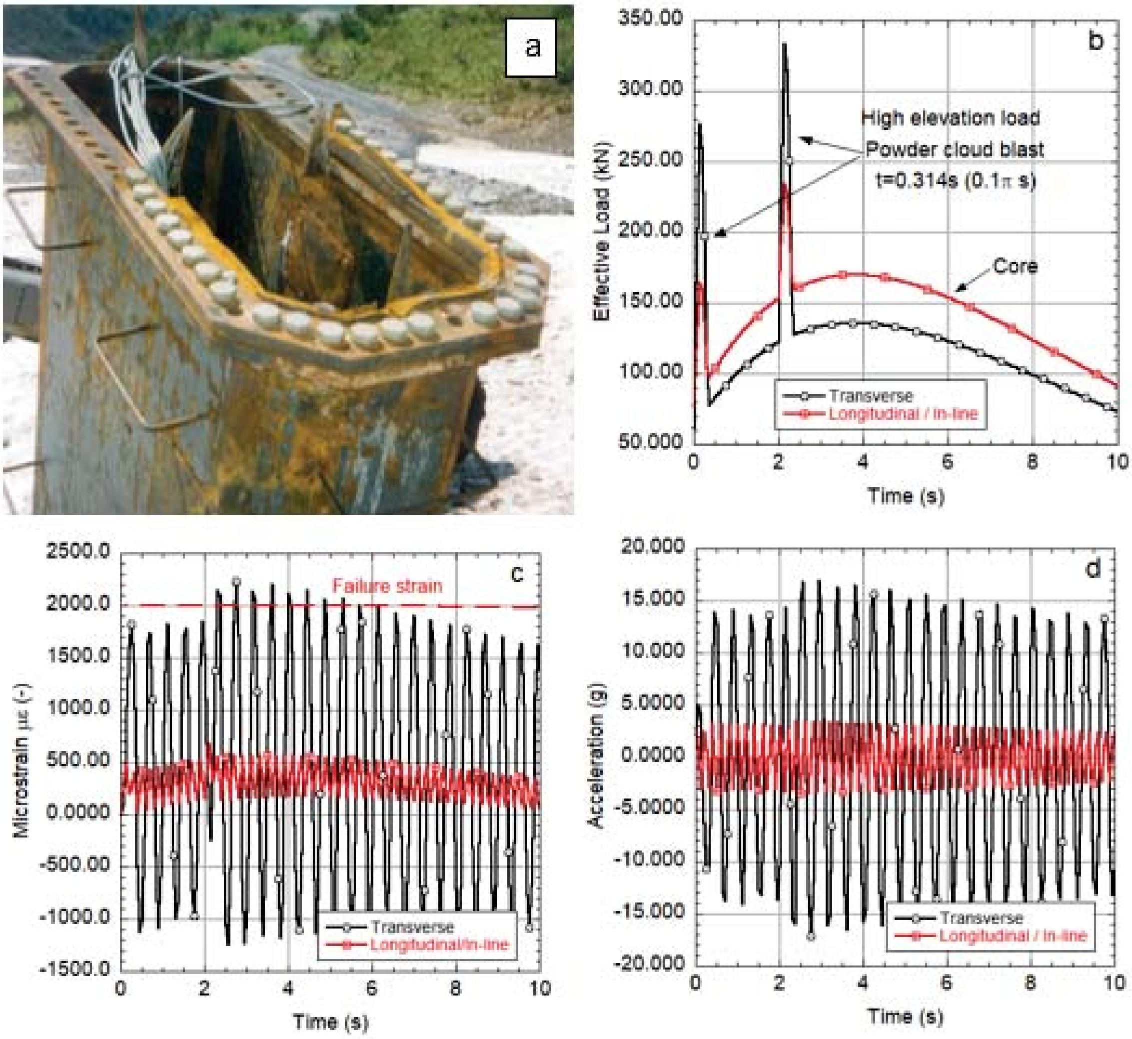

Figure 10: Results of Rayleigh analysis for the two observed avalanches with a loading duration of πs. a) Calculated microstrains for avalanche of 10.02.1999. b) Calculated effective load of 10.02.1999. c) Calculated microstrains for avalanche of 25.02.1999. The powder cloud loading excites the inertial forces such that the failure strains are reached. d) Calculated effective load of avalanche 25.02.1999.

4 CONCLUSIONS

We began our work with an analysis of measured structural accelerations induced by powder avalanche impact of a 20 m high cantilever pylon. In the measurements we could clearly identify the first three bending frequencies of the pylon in both the longitudinal and transverse directions. These eigenfrequencies could be reproduced using a simple finite element beam model. Because the pylon cross-section is a rectangular tube (1.6 m x 0.6 m, with some internal stiffening elements), the first mode eigenfrequencies differed in the longitudinal (5 Hz) and transverse (2 Hz) directions. Avalanche impact of the pylon induced accelerations reaching 10 g in the transverse direction (pylon top) and smaller accelerations in of 2 g in the stiff longitudinal direction. The significance of these results is twofold.

Firstly, a mode superposition analysis reveals that to reproduce the measured accelerations it is necessary to apply short duration blasts with duration times of approximately 0.25 s to 0.50 s. This corresponds to loading frequencies of 2 Hz to 4 Hz. At present it is not possible to model the exact timing of the blasts, but it appears there can be several within the first 10 s of the avalanche passage. It is not possible to conclude that the powder cloud contains structures only of this duration. The pylon reacts to these loading frequencies because they are near the eigenfrequencies of the pylon. It is entirely possible for the cloud to contain many different frequencies. Secondly, the powder blasts appear to be stronger than considered in the transverse direction. These transverse loadings arise as the avalanche head passes to one side of the structure. The lateral blasts are significant, especially for asymmetric structures which reduce the impact area in the longitudinal direction (in this particular case 0.6 m), but increase the length of the structure (in this particular case 1.6 m) in order to increase the flexural rigidity in the line of attack. The primary conclusion of this part of the paper is that inertial effects and dynamic magnification factors must be considered when designing pylon type structures against powder avalanche impact. Presently, this is not performed in avalanche engineering.

In the second part of the paper we performed a Rayleigh analysis of the pylon. That is, we reduced the finite element model to a single degree of system, modelling the response of the structure using only the first bending mode. In this analysis the mass, flexural rigidity and loading distributions are reduced to scalar (effective) quantities by assuming a specific deformation in the z-height direction. With this simple modelling approach, it was possible to obtain the eigenfrequencies in the longitudinal and transverse directions, but not with the accuracy of the finite element model. We simulated two large powder avalanches that occurred at the test site during the avalanche winter of 1999, on the 10.02.1999 and 25.02.1999. The second avalanche was so extreme, that it destroyed the pylon. Our analysis reveals that the transverse loading played a significant part in the structural failure, as we could only generate microstrains above the plastic limit (2000 $\mu\epsilon$) from this loading case. The first avalanche appeared to stress the pylon up to only 50% of its capacity. Of interest is the fact that the effective loading of the avalanche core contributed only 50% of the total effective loading. Moreover, the short duration powder loading, because it hits the pylon at the right frequency some distance above the ground contributes a significant part of the total effective loading.

Finally, there is considerable empirical evidence that the duration of the powder blast increases with distance from the avalanche core, where the powder cloud is formed. Trees have eigenfrequencies of approximately 1 Hz and would easily survive short duration powder blasts in the 2 Hz to 5 Hz range. This result suggests that the blast frequency of the cloud is continually changing in time and space. The powder cloud contains a wide spectrum of turbulent wavelengths that would excite tall structures. As the cloud turbulence dissipates, we expect longer duration blasts which would blow-down tree stands. This fact would explain why trees in the runout zone of avalanches (and on the sides of avalanche tracks) are especially vulnerable to the action of the powder cloud. This fact motivates our interest in understanding both the production and decay of vorticity in powder avalanches. For shear flows with varying in space and time vorticity an intermediate model was recently proposed where the governing equations are obtained by depth-avergaing the Euler equations without assuming potential flow [12, 13, 14].

REFERENCES

[1] Bozhinskiy, A. N., and Losev, K. S., The fundamentals of avalanche science, Mitt. Eidgenöss. Inst. Schnee- Lawinenforsch. 55: 280 p., 1998.

[2] P. Bartelt, A. Caviezel, M. Christen, O. Buser, Impact of hanging cables and power transmission lines by mixed flowing/powder avalanches, *25th international conference on theoretical and applied mechanics*, Milan, Italy, August 23-28, 2020.

[3] P. Bartelt, P. Bebi, T. Feistl, O. Buser and A. Caviezel, Dynamic magnification factors for tree blow-down by powder snow avalanche air blasts. *Natural Hazards and Earth System Science*, **18**(3), 759-764, 2018.

[4] Clough R. and J. Penzien, *Dynamics of Structures*. McGraw-Hill, New York, NY, 1975.

[5] W. Ammann, A new Swiss test-site for avalanche experiments in Vallée de la Sionne/Valais, Cold Regions Science and Technology, **30**(1-3), 3-11,1999.

[6] B. Sovilla, J. McElwaine and A. Köhler, The Intermittency Regions of Powder Snow Avalanches, Journal of Geophysical Research: Earth Surface, 123. https://doi.org/10.1029/2018FJ004678.

[7] http://www.fftw.org, last accessed 17.03.2021.

[8] Maple 2019. Maplesoft, a division of Waterloo Maple Inc., Waterloo, Ontario.

[9] Wolf, J.P., *Dynamic Soil Structure Interaction* Prentice-Hall, Englewood Cliffs, NJ, 1983.

[10] P. Bartelt, O. Buser, C. Vera Valero and Y. Bühler, Configurational energy and the formation of mixed flowing/powder snow and ice avalanches, **57**(71), Annals of Glaciology,179-188, 2016.

[11] L. Dreier, Y. Bühler, C. Ginzler and P. Bartelt, Comparison of simulated powder snow avalanches with photogrammetric measurements, 57(71),Annals of Glaciology, 371–381, 2016.

[12] V. M. Teshukov, Gas dynamic analogy for vortex free–boundary flows, Journal of Applied Mechanics and Technical Physics,**48**,303–309, 2007.

[13] S. Gavrilyuk, K. Ivanova, N. Favrie, Multi-dimensional shear shallow water flows: Problems and solutions, Journal of Computational Physics, **366**, 252-280, 2018.

[14] K. Ivanova, S. Gavrilyuk, Structure of the hydraulic jump in convergent radial flows. Journal of Fluid Mechanics, **860**, 441-464, 2019.